J Sol-Gel Sci Technol (2015) 74:187–198
DOI 10.1007/s10971-014-3595-y

ORIGINAL PAPER

Characterization and evaluation of silica particles coated by PVP and albumin for effective bilirubin removal

Alexander S. Timin · Alexey V. Solomonov · Irek I. Musabirov · Semen N. Sergeev · Sergey P. Ivanov · Evgeniy V. Rumyantsev

Received: 29 September 2014 / Accepted: 2 December 2014 / Published online: 12 December 2014

Abstract Polyvinylpyrrolidone (PVP) modified silica coated with albumin as host matrices for bilirubin removal were synthesized through sol–gel method. Such materials were characterized by scanning electron microscopy, nitrogen adsorption, Fourier transform spectroscopy and elemental analysis. It was shown that PVP grafted onto silica provides strong and high immobilization of BSA in comparison with pure silica. These modified silicas with different content of BSA were used to study bilirubin adsorption from the bilirubin–phosphate solutions (pH 7.4). The effect of time, ionic strength and concentration on the bilirubin adsorption were investigated as well. The results demonstrate that the adsorption capacity of tested samples increases after surface modification. The maximum adsorption capacity for bilirubin was 2.82 mg/g.

Keywords Sol–gel · Silicas · Albumin · Adsorption · Functionalization · Bilirubin

A. S. Timin (✉) · A. V. Solomonov · E. V. Rumyantsev
Department of Inorganic Chemistry, Ivanovo State University of Chemistry and Technology (ISUCT), 7, Sheremetevsky Prosp., Ivanovo, Russia
e-mail: a_timin@mail.ru

I. I. Musabirov · S. N. Sergeev
Institute for Metals Superplasticity Problems, Russian Academy of Sciences, Ufa, Russia

S. P. Ivanov
Ufa Science Centre, Institute of Organic Chemistry, Russian Academy of Sciences, Ufa, Russia

1 Introduction

Nowadays, many studies have focused on the preparation of different organo-functionalized materials for biomedical and pharmaceutical applications [1]. Moreover, drug release can be easily controlled through adjusting the structure of such organo-functionalized materials, their surface properties and particle size. Controlling the morphology and surface properties of organo-functionalized materials provides the unique physicochemical properties for biomedical applications such as sutures, artificial tissues, implants and drug delivery systems [2].

The wide potentialities of the sol–gel method in the field of surface functionalization were demonstrated by the synthesis of silica modified with different polymers [3–5]. The sol–gel method provides a possibility to design different materials keeping control over their chemical and physical properties [6]. Besides, the nature of functional groups in polymer fragment grafted onto silica surface plays an important role in morphology and interface phenomena [2, 7] that opens a great potential to use such materials in drug delivery systems or treatment of different toxicological diseases.

One of the well-known endogenous toxins is bilirubin [8]. Normally, bilirubin is conjugated with albumin forming water-soluble complex in a blood plasma [9, 10]. But a high concentration of free bilirubin in blood plasma can evoke hepatic and permanent brain damage [11]. Many techniques have been employed for removal of the high concentration of free bilirubin from plasma in order to prevent the hepatic and brain damage [11]. However, hemoperfusion treatment based on application of hemoadsorbents is one of the most effective techniques at present time [12, 13]. Thereby, the development of new approaches to improve adsorption capacity of these hemoadsorbents is actual aim.

Some researchers have prepared several adsorbents for bilirubin removal [9, 10]. In a recent paper, the novel adsorbents based on carbon nanotubes were synthesized and a good adsorption capacity for bilirubin removal was demonstrated [11]. The great potential of titania films and nanoparticles, synthesized using sol–gel technique for bilirubin adsorption, were shown as well [14–16]. Yang and his colleges prepared nanostructural hydroxyapatite for monitoring the adsorption/degradation behavior of bilirubin. [17]. We also showed in our previous work that bilirubin molecules can be easily attached to guanidine polymers via electrostatic interactions [18]. However, despite of the wide range of different valuable adsorbents, the synthesis and modification of new efficient materials for bilirubin removal is still actual purpose in a modern material science.

The sol–gel method is a well-known technique for protein immobilization [19–25]. However, some disadvantages have been found in synthesis of protein-imprinted materials associated with manipulation of protein–surface interactions [26]. The interaction between protein and silica surface might be not strong enough to prevent the protein leaching [26]. This problem can be solved using covalent immobilization (hard synthetic conditions) or via formation of a strong complex between protein and biocompatible polymers grafted onto silica surface [27–30]. Such biopolymers grafted onto silica surface can increase binding affinity to the protein.

In our study we used PVP as a biocompatible polymer which can interact with bovine serum albumin (BSA). PVP has already been used for surface modification with different materials such as metal oxide [31, 32], polystyrene [33], silica [34], graphite [35] etc. Moreover, the unique biocompatibility of PVP with different biomolecules and peptides allows to consider PVP as an effective agent in sol–gel synthesis for surface improvement [32–35].

In this study we prepared PVP-modified silica particles (PVP-MSiNs) coated with BSA (PVP-MSiNs@BSA) via a sol–gel method as effective adsorbents for bilirubin removal from aqueous solutions at pH 7.4. The preparation, characterization and application of such materials in bilirubin adsorption were presented and discussed in details. Also we compare the adsorption capacity of our materials with analogues reported in literature (Table 1).

2 Experimental section

2.1 Reagents and materials

TEOS (tetraethoxysilane, 98 %) $Si(OC_2H_5)_4$ was obtained from commercial chemical company "Ecos-1" (Russian Federation). PVP ($M_w = 10.000$ g/mol) and BSA (bovine serum albumin, $M_w = 66{,}430$ g/mol) were supplied by Sigma-Aldrich (USA). Bilirubin ($M_w = 584.7$ g/mol) was purchased from Sigma-Aldrich (USA). Aqueous solutions at pH 7.4 were prepared by dissolving bilirubin in NaOH solution, lowering the pH by addition of phosphate buffer and filtering the prepared solution to remove any solid bilirubin. Absolute ethanol, HCl and ammonia solution (25 wt % ammonia) were obtained from "Ecos-1". The chemicals were analytical grade and were used without further purification. Deionized water was used for all preparations.

2.2 Synthesis of PVP-MSiNs

A sol–gel synthesis of non-functionalized silica particles is described in [35]. In case of PVP-MSiNs, we used acid/base catalyzed sol–gel synthesis. For this reason, we divided this synthesis into two steps. In the first step, acid hydrolysis was used: 8 g of TEOS and 20 g of ethanol were mixed and then 2.8 g of H_2O containing required amount of PVP was added and stirred for 10 min. Then HCl solution was added as an acidic catalyst to adjust the pH to 5.5. We decided to prepare four water solutions containing 0.08, 0.12, 0.16 and 0.24 g of PVP, respectively. In the second step, we used basic catalyst. After hydrolysis of TEOS, ammonia solution (25 wt %

Table 1 Adsorption capacity for bilirubin of modified adsorbents from the literature

Material	Ligand (method of modification)	Adsorption capacity (mg/g)	References
Polyethyleneimine	Cyclodextrin	2.5	[36]
Chitosan particles	Poly-D-lysine	1.5	[37]
Amino-modified silica particles	Bovine serum albumin	1.17–1.65	[26]
silica particles	Polymethacrylate guanidine	0.48–0.64	[18]
Silica particles	Polyacrylate guanidine	0.94–1.10	[18]
Poly(HEMA-MAT)/MIP[a]	Molecular recognition	3.41	[9]
Cellulose acetate fiber	Cibaron Blue F3GA	4	[38]
Poly(MAA-EDGMA)/MIP[a]	Molecular recognition	1.04	[39]
PVP-MSiNs@BSA	Bovine serum albumin	1.4–2.82	This study

[a] Adsorption capacity for prepared materials, measured in mg/g

ammonia) was added to increase the pH to 8–9. The obtained solutions were stirred for 2 h until the formation the ultra-disperse silica particles. After that, the final product was transferred into a Petri dish for solvent evaporation at room temperature. The obtained samples were washed with ethanol and then with deionized water. After that, they were separated by centrifugation and dried at 95 °C under vacuum for 3 days. The acid/base catalyzed sol–gel synthesis was chosen as the most effective way for strong grafting of PVP and maximum hydrolysis of TEOS [26].

2.3 Immobilization of BSA

PVP-MSiNs (125 mg) were incubated in 10 ml of BSA solution (4 mg/ml) for 4 h at room temperature with the following centrifugation at 6,000 rpm. After that the BSA/PVP silica particles were transformed from solutions and dried under vacuum at 60 °C. Then these obtained samples were washed with 1 M NaCl and deionized water to remove unreacted BSA molecules.

BSA concentration of the solution after removing of PVP modified silica particles was determined by UV–Visible spectrophotometer SF-104 ("Aquilon", Russian Federation) at 280 nm (BSA $\varepsilon_{280} = 41{,}000$). The quantity of immobilized BSA was determined by the difference between initial and final concentrations of BSA per gram of silica and presented in mg/g.

2.4 Bilirubin adsorption measurements

The required amount of bilirubin (stored in dark at 15 °C) was dissolved in 0.2 ml of NaOH (pH = 13). After complete dissolution and intensive mixing during 5 min, it was diluted by addition of phosphate buffer (NaH_2PO_4/Na_2HPO_4, pH = 7.4) to obtain 10 ml of solution with the following filtering to remove solid bilirubin if any remained. The bilirubin solutions were also stored in the dark at 15 °C and fully uses during 2 h. Such prepared solution with required concentration of bilirubin was used for adsorption experiments.

In every experiment, 125 mg of a dry adsorbent and 10 ml of bilirubin solution were mixed and stirred at 25 °C. After the adsorption equilibrium has been attained, the solution was separated by centrifugation. The concentration of bilirubin in phosphate solution (pH 7.4) before and after adsorption was determined by UV–Visible spectrophotometer SF-104 ("Aquilon", Russian Federation) at 440 nm. The pH values were measured by a pH-meter U-500 ("Aquilon", Russian Federation). Confidence intervals of 95 % were calculated for all samples, to determine the margin of error. The amount of bilirubin adsorbed onto silica surface (mg/g) was calculated by the following equation:

$$q = \frac{V \cdot (C_o - C)}{m} \quad (1)$$

where C_o and C are the initial and the residual bilirubin concentration in solution (mg/ml), V is the volume of bilirubin solution (in ml), m is the mass of the adsorbent (in mg), respectively. Also the presence of removed bilirubin–BSA complex is detected by spectrophotometry at the wavelength of 460 nm.

2.5 Characterization techniques

Scanning electron micrographs (SEM) were performed using a high resolution scanning electron microscope Tescan Mira-3LMH operating at accelerating voltage of 20 kV. Before examining, the all samples were dissolved in ethanol. The obtained emulsion was coated onto the polished surface of aluminum table. The obtained samples were kept for a day under vacuum (10^{-2} Pa).

Specific surface area, total pore volume and average pore diameter were measured by nitrogen adsorption–desorption isotherms were measured at 77 K on a Micromeritics ASAP 2,020 m instrument (Micromeritics Instrument Corp., Norcross, GA). The pore size was calculated on the adsorption branch of the isotherms using the Barrett–Joyner–Halenda method and specific surface area was calculated using the Brunauer–Emmett–Teller (BET) method. Error in determining of a BET surface area and pore volume are estimated to be within 5 %.

Fourier transform infrared (FT-IR) spectra of the samples were performed on a NicoletTM 4700 FTIR spectrometer ("Nicolet", USA) using KBr technique. The nitrogen, hydrogen and carbon contents were determined by an Elemental Analyser (Thermo Flash 1112 CHNS Analyzer).

3 Results

The elemental analysis of PVP-MSiNs was carried out to confirm the presence of PVP after sol–gel synthesis and thermal/ethanol treatments (Table 2). The results proved that PVP was successfully grafted on silica surface. We also determined the grafting degree (GD) of PVP onto silica surface from the nitrogen content. As it can be seen the grafting degree of PVP increases from 0.68 to 1.84 wt% which is logically in agreement with initial conditions of synthesis.

The nitrogen adsorption–desorption isotherms of all prepared samples are shown in Fig. 1. The pure silica (SiN) and PVP-MSiNs exhibit type I and type IIb isotherms according to the IUPAC classification [26]. The typical hysteresis loops (type H3) are observed in case of PVP-MSiNs associated to inter-particles pores originating from packing of particles. The BET surface area of all samples

Table 2 Physical properties of the obtained samples

Sample	BET surface area[a] (m^2/g)	Total pore Volume[b] (cm^3/g)	Average pore size[c] (nm)	Elemental composition (wt%)[d]			
				C	H	N	GD of PVP (%)[e]
SiN	40	0.015	2.5	–	–	–	–
PVP-MSiN-1	106	0.65	33.2	3.51	0.47	0.68	5.71
PVP-MSiN-2	131	0.75	51.5	5.12	0.65	0.99	8.53
PVP-MSiN-3	143	1.12	54.4	6.54	0.85	1.29	11.41
PVP-MSiN-4	152	1.19	31.6	9.48	1.20	1.84	17.10

[a] BET specific surface area measured in the 0.05–0.25 range of the relative pressures

[b] Total pore volume was calculated at a relative pressure about 0.99

[c] Average pore size was calculated from the BJH method (4 V/A)

[d] Elemental analysis was performed via Elemental Analyser (Thermo Flash 1112 CHNS Analyzer)

[e] Determined using eq. $GD = \frac{w(N)\cdot M(PVP)/M(N)}{(1-w(N)\cdot M(PVP)/M(N))} \times 100$ where w(N) is the content of nitrogen in prepared sample; M(PVP) and M(N) are molecular weights of repeating monomer in PVP chain and nitrogen, respectively

along with their total pore volume and average pore size calculated according to the BJH methods are listed in Table 2. The obtained results show that the surface properties of PVP-MSiNs are clearly different from SiN. The SiN is characterized by a low specific surface area ($\sim$40 m^2/g). Also the pore size distribution curve of pure silica shows very intensive peak at 2.6 nm and one weak peak between 5 and 7 nm. However, the increase in the surface area, pore size and pore volume is observed after surface functionalization for all silicas modified with different grafting amount of PVP. This fact confirmed a big impact of PVP on surface properties of silica nanoparticles.

3.1 Structural and textural characterization of the obtained materials

The structure of PVP-MSiNs was characterized using SEM analysis. The SEM images of SiN was shown and discussed in our previous work [26]. The particles of SiN have a spherical shape and range from 200 to 300 nm. The particles are well defined and do not form agglomerates. The SEM images of PVP-MSiNs (Fig. 2) show the presence of particles agglomerates ranging in size from 200 nm to 2 μm. It's obvious that these cluster agglomerates consist of uniform spherical nanoparticles when the magnification is increased. This fact confirmed an important influence of PVP on morphology of the final product. The particle size distribution was also obtained. About 1,000 particles (agglomerates and individuals) of each sample were analyzed and then the histograms of particle size distribution were built. From the obtained histograms we can suggest that if the amount of PVP is increased, the main peak (average particle size) is shifted to large particles.

3.2 Immobilization of BSA

Experiments involving the BSA immobilization for SiN and PVP-MSiNs were conducting for an initial concentration of BSA (4 mg/ml) at room temperature. As it can be observed from Fig. 3a, the amount of immobilized BSA increased with increasing the quantity of PVP incorporated inside the silica matrix. The maximum amount of BSA adsorbed on unmodified silica was 26 mg/g, whereas using PVP as an agent for surface modification, 72 mg/g was achieved.

It was performed desorption studies in order to remove extra quantity of BSA from silica surface. For this reason BSA modified silicas were washed in 10 ml of phosphate buffer and then in 1 mol/L NaCl solution. Desorption process was repeated until the removing of BSA has stopped. Figure 3b shows the BSA desorption capacity as a function of time for all tested samples. The equilibrium amount of desorbed BSA for unmodified silica was about 54 % whereas it was about from 25 to 19 % of adsorbed BSA is desorbed from PVP-MSiNs. It was managed to reduce the release of large quantity of BSA from silica matrix using PVP. Desorption of BSA most probably occurs due to the increase of ionic strength (influence of NaCl) which leads to a decrease of electrostatic interaction between PVP and BSA.

Thus, after desorption studies we can conclude that only 14 mg/g of BSA was managed to strongly load on silica surface without any further leaching in case of unmodified silica. As for PVP-MSiNs, the amount of BSA grafted onto modified silica surface after the removal procedure was 28 mg/g (PVP-MSiN-1), 35 mg/g (PVP-MSiN-2), 43 mg/g (PVP-MSiN-3) and 53 mg/g (PVP-MSiN-4), respectively. Then, we use final products with different quantity of BSA grafted onto silica surface to investigate bilirubin adsorption from phosphate buffer at pH 7.4.

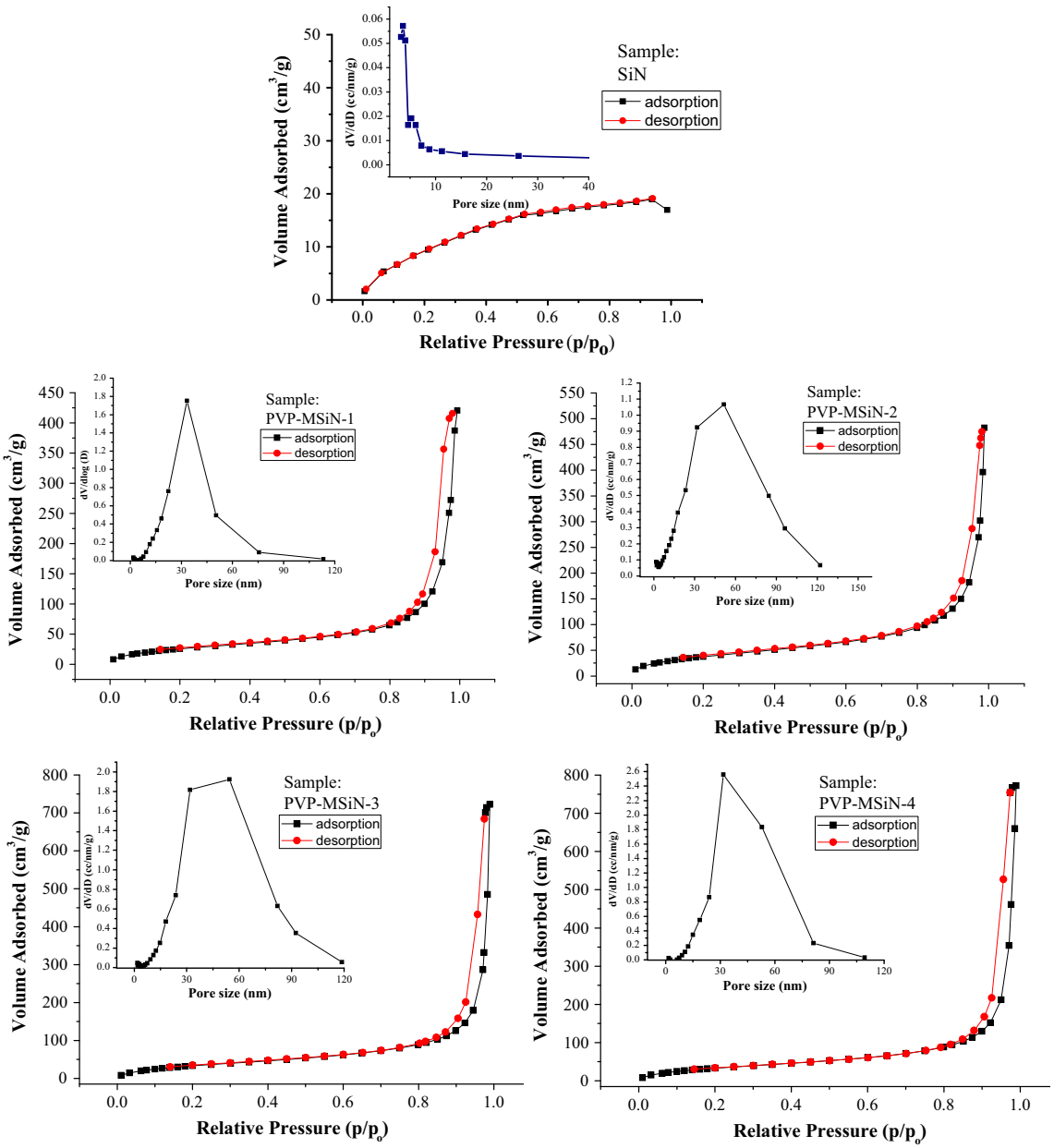

Fig. 1 Nitrogen adsorption/desorption isotherms at 77 K of the obtained samples with corresponding the pore size distribution (*inset*)

3.3 Adsorption rate of bilirubin

The effect of time on bilirubin adsorption was studied. Figure 4 demonstrates the specific adsorption rate curves of bilirubin for SiN and PVP-MSiNs@BSA. Also it should be mentioned that water-soluble complex of BSA with bilirubin can be detected by spectrophotometry at the wavelength of 460 nm. The presence of such peak at 460 was not observed for all albumin containing samples which confirmed the fact of the strong BSA immobilization onto silica surface after adsorption/desorption process. As it can be observed, the BSA immobilization onto the silica surface leads to the increase of adsorption capacity for bilirubin in comparison with pure unmodified silica. The amount of adsorbed bilirubin onto the surface of SiN is quite low (0.32 mg/g) whereas the adsorption capacity of BSA-immobilized silica (SiN@BSA) is higher and equals 0.59 mg/g. The adsorption capacity of PVP-MSiNs@BSA ranges from 1.4 to 2.82 mg/g. It is obvious that such values of adsorption capacity are higher than in the case of SiN and SiN@BSA. However, the adsorption kinetics of SiN and SiN@BSA was faster than for the

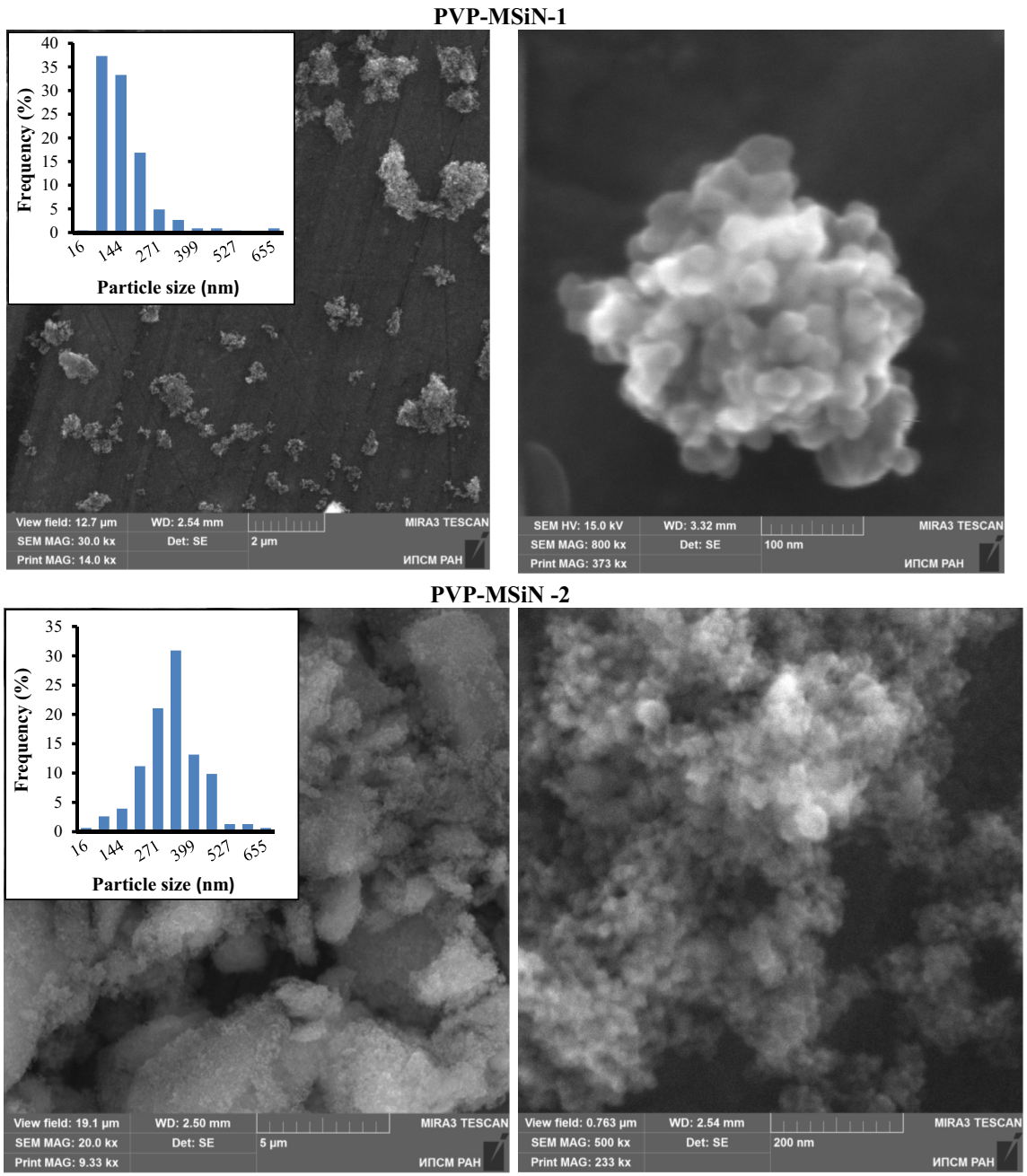

Fig. 2 SEM micrographs of PVP-MSiNs and corresponding histograms of particle size distribution (*inset*)

PVP-MSiNs@BSA. The required time to reach equilibrium conditions was approximately 60 min in case of SiN and SiN@BSA whereas the adsorption time of PVP-MSiN-1@BSA (28 mg/g) and PVP-MSiN-2@BSA (35 mg/g) was ~90 min. It takes more contacting time (~120 min) in order to reach the maximum adsorption capacity for PVP-MSiN-3@BSA (43 mg/g) and PVP-MSiN-4@BSA (53 mg/g). These results indicate that the adsorption rate of bilirubin depends on the amount of incorporated PVP and BSA, respectively.

The adsorption kinetic models (pseudo first- and second-order equations) were used to study the adsorption rate that controls the residence time of adsorbate uptake at the solid-solution interface. The first-order rate equation of Lagergren is generally expressed as follows:

$$\log(q_e - q_t) = \log(q_{1cal}) - \frac{k_1 \cdot t}{2.303} \quad (2)$$

where q_e and q_t are the adsorption capacity at equilibrium and at time t, respectively (mg/g), k_1 is the rate constant of

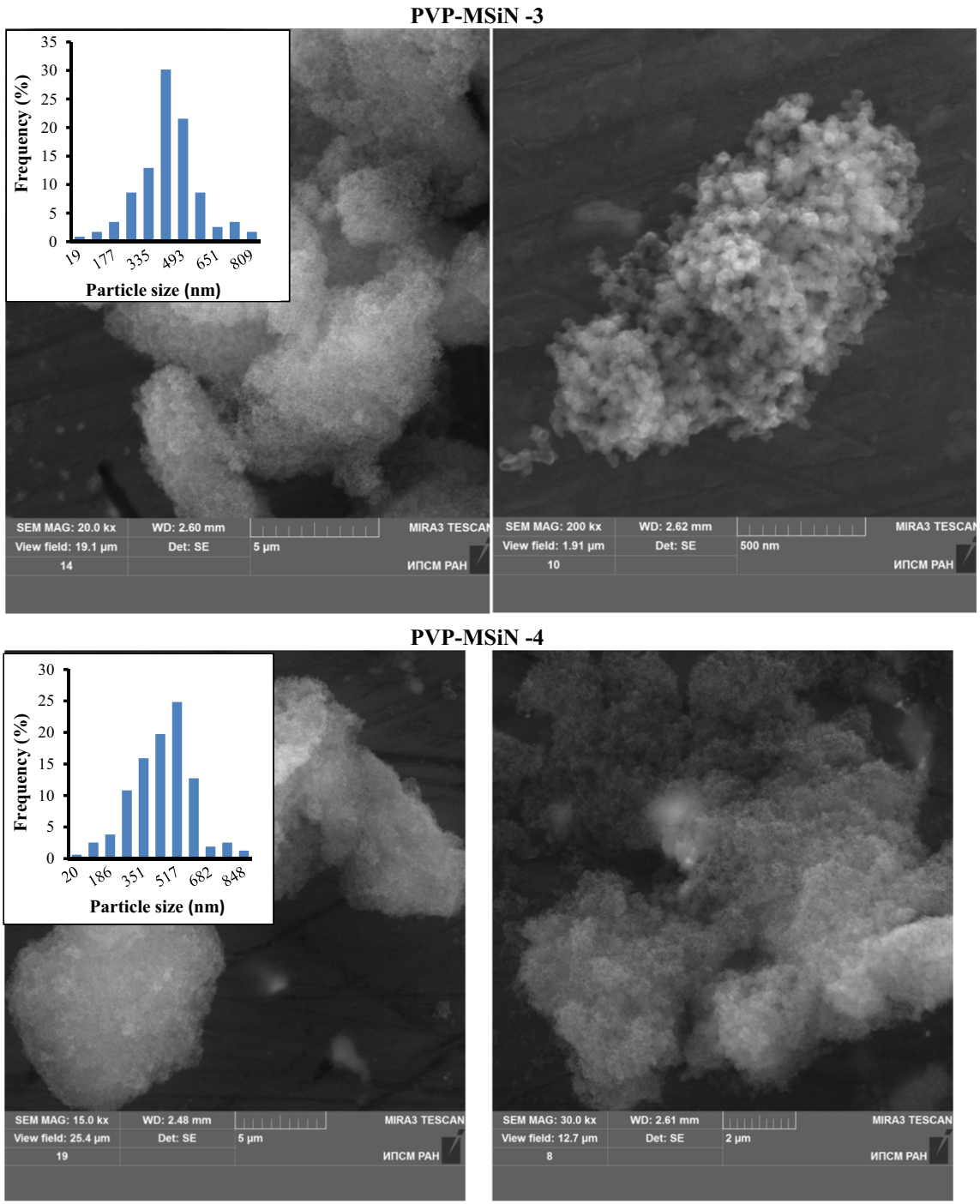

Fig. 2 continued

pseudo first-order adsorption (1/min), q_{1cal} is the adsorption capacity calculated by pseudo first-order model (mg/g)

The linear form of the pseudo second-order equation can be represented as follows:

$$\frac{t}{q_t} = \frac{1}{k_2 q_{2cal}^2} + \frac{1}{q_{2cal}} t \quad (3)$$

where k_2 is the rate constant of pseudo second-order adsorption (1/min) and q_{2cal} is the adsorption capacity calculated by pseudo second-order model (mg/g).

The results for the first-order and second-order kinetics models are listed in Table 3. R^2 values for second-order equation are higher than in case of R^2 values of first-order

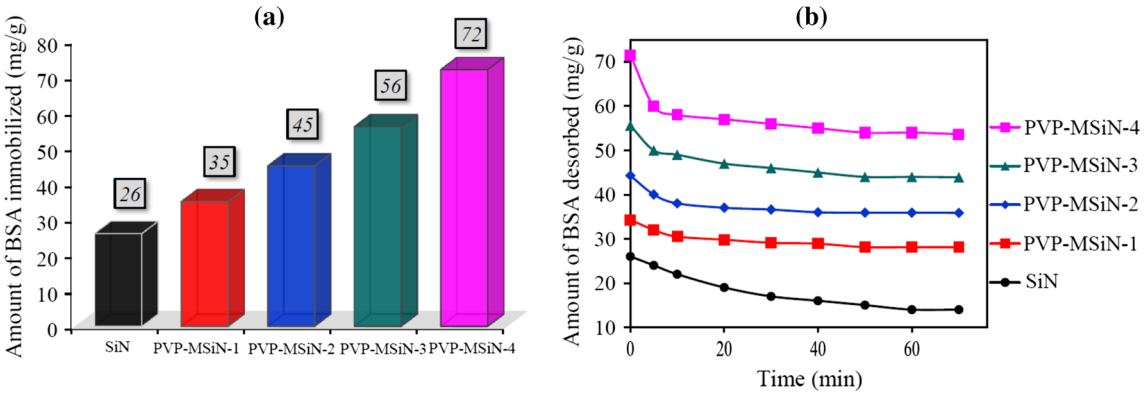

Fig. 3 Influence of the quantity of grafted PVP on BSA immobilization (**a**); BSA desorption as function of time for SiN and PVP-MSiNs; $V = 10$ ml; $m = 125$ mg adsorbent, and $T = 25$ °C

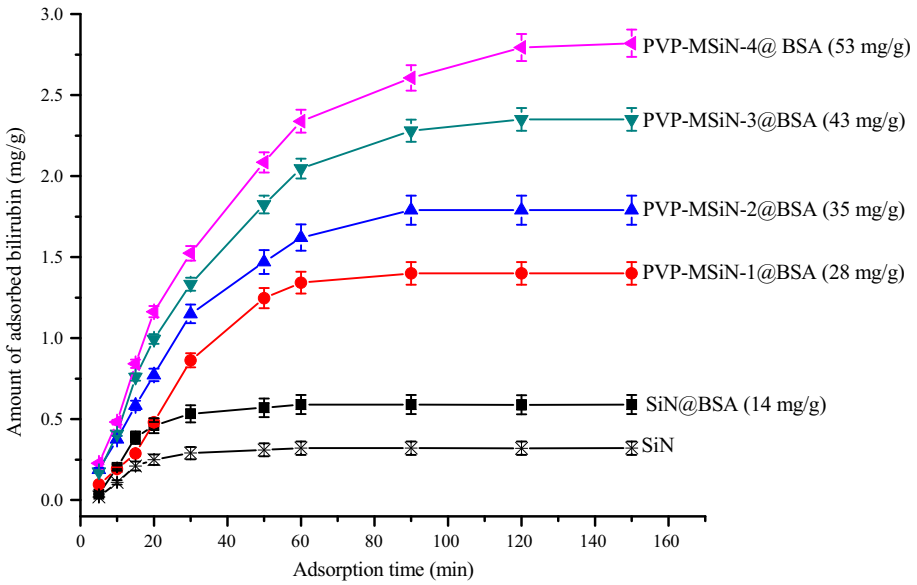

Fig. 4 Effect of time on the adsorption of bilirubin at pH 7.4 (phosphate buffer) by SiN and PVP-MSiNs; $V = 10$ ml; $m = 125$ mg adsorbent, and $T = 25$ °C

equation indicating that second-order mechanism is predominant.

3.4 Effect of equilibrium concentration of bilirubin

The relations between the equilibrium concentration of bilirubin and equilibrium adsorption for all tested samples are given in Fig. 5. The shape of isotherms for all tested samples is very familiar. The adsorption values of bilirubin increased as the bilirubin concentration increased, and finally reached a saturation level at high concentrations. It can be seen that up to a certain concentration, no more bilirubin can be adsorbed on the silica surface. As it was shown in the section "bilirubin adsorption rate", the BSA immobilization increases the adsorption ability to bilirubin. Also the adsorption capacity of PVP-MSiNs@BSA is found to be much higher in comparison with SiN and SiN@BSA. It is clear that adsorption capacity increased with increasing amount of BSA immobilized onto silica surface.

Langmuir and Freundlich adsorption models have been used for analysis of the experimental data. The Langmuir and Freundlich equations are

$$q = \frac{q_{\max} K_d C_e}{1 + K_d C_e} \tag{4}$$

$$q = K_F C_e^{1/n} \tag{5}$$

where C_e is the equilibrium concentration of bilirubin, q_{max} is the maximum adsorption according to the Langmuir model, K_d and K_F are the Langmuir and Freundlich constants, respectively, n is the Freundlich exponent.

Table 4 shows all calculated parameters for Langmuir and Freundlich models. According to the correlation coefficients of isotherms, the adsorption data fit the Langmuir isotherm equation best, followed by the Langmuir isotherm.

Table 3 First- and second-order kinetics constants for all tested samples

Sample	Exp	First-order kinetics			Second-order kinetics		
	q_{eq} (mg/g)	k_1 (1/min)	q_{cal} (mg/g)	R^2	k_2	q_{2cal}	R^2
SiN	0.32	0.0737	0.37	0.974	0.2797	0.35	0.989
SiN@BSA (14 mg/g)	0.59	0.0738	0.69	0.975	0.1524	0.64	0.984
PVP-MSiN-1@BSA (28 mg/g)	1.41	0.0345	1.72	0.928	0.0164	1.81	0.985
PVP-MSiN-2@BSA (35 mg/g)	1.79	0.0368	2.02	0.985	0.0167	2.19	0.986
PVP-MSiN-3@BSA (43 mg/g)	2.35	0.0391	2.90	0.986	0.0084	3.08	0.991
PVP-MSiN-4@BSA (53 mg/g)	2.82	0.0369	3.71	0.965	0.0061	3.77	0.989

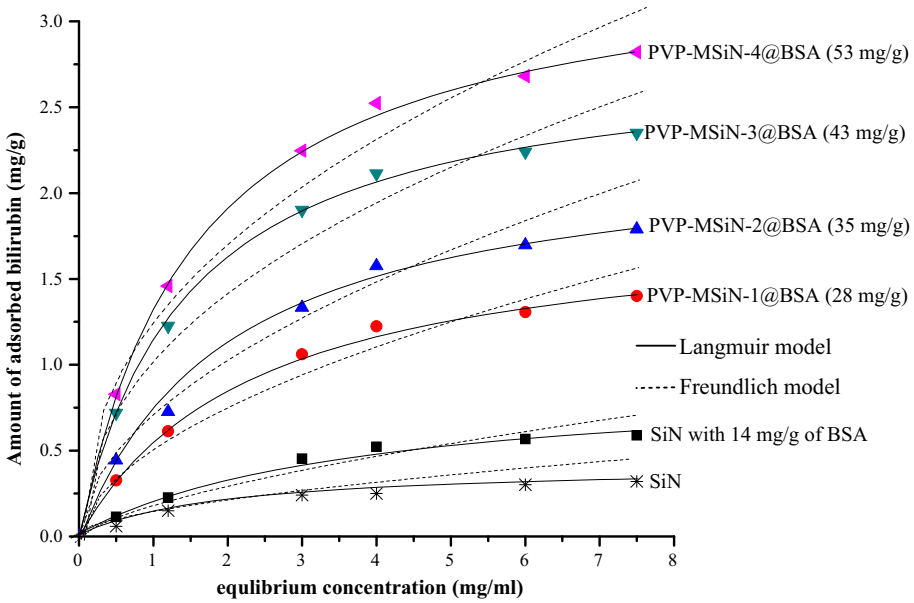

Fig. 5 Experimental adsorption isotherms of bilirubin for SiN and PVP-MSiNs@BSA; $V = 10$ ml; $m = 125$ mg adsorbent, and $T = 25$ °C; adsorption time = 2 h

Table 4 Langmuir and Freundlich adsorption isotherm parameters

Sample	Exp	Langmuir Model			Freundlich Model		
	q_{eq} (mg/g)	q_{max} (mg/g)	K_d	R^2	K_F	n	R^2
SiN	0.32	0.39	0.51	0.992	0.11	1.68	0.944
SiP@BSA (14 mg/g)	0.59	0.94	0.28	0.985	0.19	1.59	0.946
PVP-MSiN-1@BSA (28 mg/g)	1.41	1.86	0.42	0.999	0.52	1.84	0.945
PVP-MSiN-2@BSA (35 mg/g)	1.79	2.21	0.49	0.987	0.67	1.86	0.944
PVP-MSiN-3@BSA (43 mg/g)	2.35	2.81	0.68	0.998	1.06	2.27	0.941
PVP-MSiN-4@BSA (53 mg/g)	2.82	3.42	0.64	0.999	1.25	2.20	0.941

3.5 Effect of ionic strength on bilirubin adsorption

The effect of ionic strength on the bilirubin adsorption was investigated because the ionic strength is one of the major factors that has an impact on the adsorption process (Fig. 6). We perform this experiment for all samples excepting SiN because such sample is characterized by low adsorption capacity for bilirubin and is not interesting for the following consideration. The obtained results show that adsorption behavior of bilirubin was strongly affected by concentration of NaCl in bilirubin solution. The adsorption capacity for bilirubin decreased as NaCl concentration increased. The explanation of such phenomenon is discussed below.

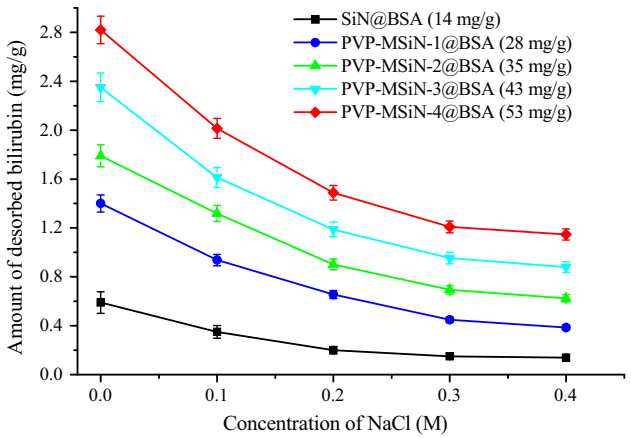

Fig. 6 Effect of NaCl concentration on bilirubin adsorption for BSA modified samples; $V_{total} = 10$ ml, $m_{ads} = 125$ mg, pH 7.4 (phosphate buffer), $T = 26$ °C

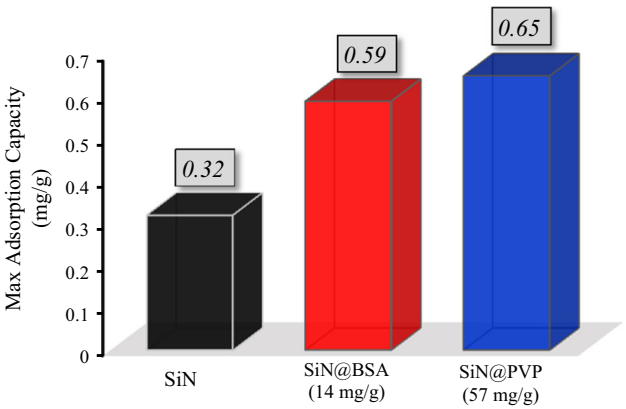

Fig. 7 Comparison in adsorption capacity of SiN, BSA- and PVP-grafted silicas towards bilirubin

4 Discussion

Our work can be basically divided into two distinct parts. In the first part we present a full characterization of functionalized silica particles and the influence of PVP on BSA immobilization. Here we show that PVP grafting during the sol–gel synthesis leads to the formation of big clusters of agglomerates. This fact might be explained by the formation of additional electrostatic interactions between Si and O^- and positively charged nitrogen in PVP chain during sol–gel process [40]. It might have a negative side on modification of silica particles using PVP. However, we showed that PVP grafting plays an important role in protein immobilization. According to the process of BSA immobilization, the porous channels of silica are full of PVP that makes it valuable to interact with BSA to form interconnected complexes. The large pores in PVP modified silicas allow the BSA molecules to diffuse in materials and interact with incorporated PVP via electrostatic and H-bond interactions that provide additional binding with BSA. Also hydrophobic/phydrophilic forces positively influence the BSA immobilization [41, 42]. The unmodified silica is characterized by a low adsorption capacity compared to PVP modified silicas due to the low surface area and pore size. Only Si–OH/Si–O^- groups on the inner walls of silica channels facilitate the protein immobilization. Moreover, PVP grafting does not only increase the loading efficiency for BSA but also provides stronger binding of BSA molecules with silica surface compared to unmodified silica. We also proved the successful immobilization of BSA onto silica surface via a physical adsorption process using FTIR spectroscopy. The FTIR spectra of SiN and PVP-MSiNs with physically adsorbed BSA revealed two very intensive peaks at 1,656 and 1,533 cm^{-1} corresponding to the amide-I and amide-II bands, respectively [43, 44].

In the second part we applied our adsorbents to study bilirubin adsorption. Two major aspects in bilirubin adsorption are involved. One of them is the adsorption kinetics and another one is an equilibrium adsorption. According to the study of adsorption kinetics of bilirubin we demonstrated that it is required more time to reach equilibrium conditions in case of BSA/PVP-MSiNs. This is probably due to the fact that bilirubin adsorption is a very complex process which involves several factors: complexation rate of BSA with bilirubin and PVP, respectively, and diffusion stage as well. Also the content of PVP (discussed below), the geometric affinity between PVP and BSA, the specific Van der Waals interactions and electrostatic forces have significant effect on the adsorption rate of bilirubin. Moreover, we showed that the pseudo second-order mechanism is dominant and, therefore, we suggest that chemisorption is the rate-limiting step controlling the adsorption process. A wide range of adsorption rates have been reported in the literature. From the analysis of literature [44] for patients diagnosed as having fulminant hepatitis it was reported that the effective treatment time for bilirubin removal ranges from 1 to 2 h. In this study it can be concluded that the time to reach equilibrium conditions seems to be quite suitable for all tested samples.

Our study of bilirubin adsorption at equilibrium conditions demonstrates how the modification of silica particles using PVP and BSA can significantly improve the adsorption capacity for bilirubin. There are three major aspects which play a significant role in bilirubin adsorption such as the amount of immobilized BSA, the quantity of PVP grafted onto silica and the surface properties (specific surface area and pore size). We studied the equilibrium adsorption of bilirubin using PVP modified silica in order to compare the influence of PVP on bilirubin adsorption. The

diagram (Fig. 7) shows a comparison in bilirubin adsorption for SiN, MSiN@PVP (57 mg/g) and MSiN@BSA (14 mg/g), respectively. As it can be seen, the adsorption capacity is also increased after PVP grafting. However, it is required a much higher quantity of PVP to achieve the adsorption capacity which is a bit higher in comparison with the adsorption capacity of BSA modified silica. We may conclude that PVP grafting has definitely an influence on bilirubin adsorption but it is not as big as in the case of BSA molecules. As reported above, BSA molecules can form a strong complex with bilirubin providing a great increase in adsorption capacity for bilirubin [43]. The formation of intermolecular complex between bilirubin and BSA occur via different interactions: electrostatic, H-bonds, non-specific Van der Waals, hydrophobic and hydrophilic forces [57]. But in case of PVP, interactions with bilirubin can occur only via hydrogen bonding of C=O in PVP and carboxyl and imine groups in bilirubin molecular.

The last factor which has an impact on additional bilirubin binding is an increase in specific surface area and pore size. The larger pore size in case of PVP modified silicas provides a much more expeditious pathway and available pore volume for bilirubin transfer and interactions with BSA.

As mentioned in the introduction, a wide range of adsorption capacity was reported in literature for bilirubin removal (Table 1). According to our study we can conclude that our prepared adsorbents have a good adsorption capacity for bilirubin. Usually, the adsorption capacity of each modified material depends on the type of reactive ligand or functional groups grafted onto surface. For instance, the adsorption capacity of cyclodextrin modified with polyethyleneimine is a bit higher than that of our functionalized silicas. But our adsorbents have higher adsorption capacity compared to poly-D-lysine immobilized chitosan particles [37]. In our previous work, we also used amino-modified silicas with the following application of these materials for bilirubin removal and the obtained adsorption capacity for bilirubin was 1.17–1.65 mg/g [26]. As discussed above, many chemical interactions (universal and specific) between BSA and bilirubin take place. However, electrostatic interactions are the main driving forces providing a strong binding of bilirubin to BSA: the negatively charged carboxyl groups of bilirubin can be easily attached to the positively charged functional groups of constituent amino acids in BSA molecules [45]. Therefore, the increase of the ionic strength (NaCl concentration) leads to the decrease in the adsorption capacity due to the weakening of the electrostatic interaction between bilirubin and BSA immobilized onto PVP modified silicas.

5 Conclusions

We prepared new adsorbents based on silica particles modified with BSA and PVP. It was shown that the morphology and surface properties of modified silicas were tunable by the amount of incorporated PVP. Structural changes and protein immobilization ability before and after PVP grafting were determined. It was demonstrated that the adsorption capacity of each adsorbent is affected by the presence of BSA and PVP as well. However, we proved that the content of BSA immobilized onto silica surface plays the most significant role in bilirubin adsorption. The sample with the maximum content of BSA showed a good adsorption capacity for bilirubin compared to other available analogues. Therefore, this type of adsorbents could be designed as hemoadsorbents for further improvement of hemoperfusion system.

Acknowledgments We are grateful for the support via a stipend of the President of the Russian Federation for a study abroad in 2014–2015 (http://www.president-mobility.ru/node/14) and the Ministry of Education and Science of the Russian Federation, a bursary of the President of the Russian Federation (No. SP-6898.2013.4) for young scientists and graduate students engaged in advanced research and development in priority directions of modernization of Russian economics (2013–2015), and a grant of the Jewish agency for Israel and the government of Israel No. 1504994 (2014–2015).

References

1. Panyam J, Labhasetwar V (2003) Biodegradable nanoparticles for drug and gene delivery to cells and tissue. Adv Drug Deliv Rev 55:329–347
2. Xiaoguang L, Shishuai S, Fengxiang W (2014) Construction of nanoparticles based on amphiphilic compolymers of poly(y-glutamic acid co-L-lactide)-1,2-dipalmitoyl-sn-glycero-3-phosphoethanolamine as a potential drug delivery carrier. J Colloid Interface Sci 413:54–64
3. Dabrowski A, Barczak A, Dudarko OA (2007) Sol–gel approaches to materials for having covalently attached phosphonic groups. Pol J Chem 81:475–483
4. El-Nahhal IM, El-Ashgar NM (2007) A review on polysiloxane-immobilized ligand systems: synthesis, characterization and application. J Organomet Chem 692:2861–2870
5. Li XG, Ma XL, Sun J, Huang MR (2009) Powerful reactive sorption of silver(I) and mercury(II) onto poly(o-phenylenediamine) microparticles. Langmuir 25:1675–1684
6. Dudarko OA, Zub YuL, Dabrowski A (2011) Template synthesis of mesoporous silicas containing phosphonic groups. Glass Phys Chem 6:596–602
7. Nabanita P, Bhaumik A (2013) Soft templating strategies for the synthesis of mesoporous materials: inorganic, organic–inorganic hybrid and pure organic solids. Adv Colloid Interface Sci 189–190:21–41

8. Zunszain PA, Ghuman J, McDonagh AF, Curry S (2008) Crystallographic analysis of human serum albumin complexed with 4Z,15E-Bilirubin-IXα. J Mol Biol 381:394–406
9. Baydemir G, Andac M, Bereli N et al (2007) Selective removal of bilirubin from human plasma with bilirubin-imprinted particles. Ind Eng Chem 46:2843–2852
10. Lee KH, Wendon J, Lee M (2002) Predicting the decrease of conjugated bilirubin with extracorporeal albumin dialysis MARS using the predialysis molar ratio of conjugated bilirubin to albumin. Liver Trans 8:591–593
11. Limin G, Lingxia Z, Jiamin Z, Jian Z et al (2009) Hollow mesoporous carbon spheres—an excellent bilirubin adsorbent. Chem Commun 40:6071–6073
12. Holubek WJ, Hoffman RS, Goldfarb DS, Nelson LS (2008) Use of hemodialysis and hemoperfusion in poisoned patients. Kidney Int 74:1327–1334
13. Tyagi PK, Winchester JF, Feinfeld DA (2008) Extracorporeal removal of toxins. Kidney Int 74:1231–1233
14. Asano T, Tsuru K, Hayakawa S, Osaka A (2008) Bilirubin adsorption property of sol–gel-derived titania particles for blood purification therapy. Acta Biomater 4:1067–1072
15. Yang Z, Si S, Fung Y (2007) Bilirubin adsorption on nanocrystalline titania films. Thin Solid Films 515:3344–3351
16. Z-p Y, Yanb J, Zhanga C, Luo S (2011) Enhanced removal of bilirubin on molecularly imprinted titania film. Colloids Surf B 87:187–191
17. Yang Z, Zhang C (2009) Adsorption and photocatalytic degradation of bilirubin on hydroxyapatite coatings with nanostructural surface. J Mol Catal A Chem 302(1–2):107–111
18. Timin AS, Solomonov AV, Rumyantsev EV (2014) Polyacrylate guanidine and polymethacrylate guanidine as novel cationic polymers for effective bilirubin binding. J Polym Res 21:400–409
19. Wu H, Tian Y, Liu B, Lu H, Wang X, Zhai J, Jin H, Yang P, Xu Y, Wang HJ (2004) Titania and alumina sol–gel-derived microfluidics enzymatic-reactors for peptide mapping: design, characterization, and performance. Proteome Res 3:1201–1209
20. Pandey et al (1992) Amperometric enzyme sensor for glucose based on graphite paste-modified electrodes. Appl Biochem Biotechnol 33:139–144
21. Camarero JA (2008) Recent developments in the site-specific immobilization of proteins onto solid supports. Biopolymers 90(3):450–458
22. William H, Scouten JHT, Luong R, Stephen B (1995) Enzyme or protein immobilization techniques for applications in biosensor design. Trends Biotechnol 13(5):178–185
23. Krysteva et al (1991) Covalent binding of enzymes to synthetic membrane containing acrylamide units, using formaldehyde. Biotechnol Appl Biochem 13:106–111
24. Sumitra D, Christena LR, Rajaram YRS (2013) Enzyme immobilization: an overview on techniques and support materials. Biotech 3(1):1–9
25. Rusmini F, Zhong Z, Feijen J (2007) Protein immobilization strategies for protein biochips. Biomacromolecules 8(6):1775–1789
26. Timin AS, Rumyantsev EV, Solomonov AV (2014) Synthesis and application of amino-modified silicas containing albumin as hemoadsorbents for bilirubin adsorption. J Non Cryst Solids 385:81–88
27. Alberti K, Davey RE, Onishi K, George S, Salchert K, Seib FP, Bornhäuser M, Pompe T, Nagy A, Werner C, Zandstra PW (2008) Functional immobilization of signaling proteins enables control of stem cell fate. Nat Methods 5:645–650
28. Borrebaeck CA (2000) Antibodies in diagnostics—from immunoassays to protein chips. Immunol Today 21(8):379
29. Choi UB, Weninger KR, Bowen ME (2012) Immobilization of proteins for single-molecule fluorescence resonance energy transfer measurements of conformation and dynamics. Methods Mol Biol 896:3–20
30. Israelachvili JN (2010) Intermolecular and surface forces, 3rd edn. Academic Press, Waltham
31. Pattanaik M, Bhaumik SK (2000) Adsorption behaviour of polyvinyl pyrrolidone on oxide surfaces. Mater Lett 44:352–360
32. Smith JN, Meadows J, Williams PA (1996) Adsorption of polyvinylpyrrolidone onto polystyrene latices and the effect on colloid stability. Langmuir 12:3773–3778
33. Esumi K, Matsui H (1993) Adsorption of non-ionic and cationic polymers on silica from their mixed aqueous solutions. Colloids Surf A 80:273–278
34. Otsuka H, Esumi K (1995) Interaction between poly(N-vinyl-2-pyrrolidone) and anionic hydrocarbon/fluorocarbon surfactant on hydrophobic graphite. J Colloid Interface Sci 170:113–119
35. Timin AS, Rumyantsev EV (2013) Sol–gel synthesis of mesoporous silicas containing albumin and guanidine polymers and its application to the bilirubin adsorption. J Solgel Sci Technol 67:297–303
36. Limin G, Lingxia Z, Jiamin Z, Jian Z et al (2009) Hollow mesoporous carbon spheres—an excellent bilirubin adsorbent. Chem Commun 40:6071–6073
37. Chandy T, Sharma CP (1992) Polylysine-immobilized chitosan beads as adsorbents for bilirubin. Artif Organs 16:568
38. Ma Z, Kotaki M, Ramakrishna S (2005) Electrospun cellulose nanofiber as affinity membrane. J Membr Sci 265:115–123
39. Syu MJ, Deng JH, Nian YM, Chiu TC, Wu AH (2005) Binding specificity of alpha-bilirubin-imprinted poly(methacrylic acid-co-ethylene glycol dimethylacrylate) toward alpha-bilirubin. Biomaterials 26:4684
40. Chatterjee S, Prajapati R, Bhattacharya A, Mukherjee TK (2014) Microscopic evidence of "necklace and bead"-like morphology of polymer-surfactant complexes: a comparative study on poly(vinylpyrrolidone)-sodium dodecyl sulfate and poly(diallyldimethylammonium chloride)-sodium dodecyl sulfate systems. Langmuir 30:9859–9865
41. Gao Q, Xu W, Xu Y, Wu D, Sun Y, Deng F, Shen WJ (2008) Amino acid adsorption on mesoporous materials: influence of types of amino acids, modification of mesoporous materials, and solution conditions. Phys Chem B 112:2261
42. Deere J, Magner E, Wall JG, Hodnett BK (2002) Adsorption and activity of proteins onto mesoporous silica. J Phys Chem B 106:7340
43. Deere J, Magner E, Wall JG, Hodnett BK (2002) Adsorption and activity of proteins onto mesoporous silica. J Phys Chem B 106:7340
44. Zhang Q, Ge J, Yin Y (2008) Permeable silica shell through surface-protected etching. Nano Lett 8:2867–2871
45. Cunfeng S, Aifeng Zh, Wei S, Hairong J, Dongtao G (2011) Functionalized silica nanotubes as affinity matrices for bilirubin removal. Trans Nanotechnol 10(3):1–6